ACS APPLIED MATERIALS & INTERFACES

Research Article

www.acsami.org

# Highly Efficient Red-Emitting Hybrid Polymer Light-Emitting Diodes via Förster Resonance Energy Transfer Based on Homogeneous Polymer Blends with the Same Polyfluorene Backbone

Bo Ram Lee,[†,‡] Wonho Lee,[§] Thanh Luan Nguyen,[§] Ji Sun Park,[⊥] Ji-Seon Kim,[∥,○] Jin Young Kim,[▽] Han Young Woo,*[,§] and Myoung Hoon Song*[,†,‡]

[†]School of Mechanical and Advanced Materials Engineering/Low Dimensional Carbon Materials Center, Ulsan National Institute of Science and Technology (UNIST), Banyeon-ri 100, Ulsan 689-798, Republic of Korea

[‡]KIST-UNIST Ulsan Center for Convergent Materials, Ulsan National Institute of Science and Technology (UNIST), Banyeon-ri 100, Ulsan 689-798, Republic of Korea

[§]Department of Cogno-Mechatronics Engineering (WCU), Pusan National University, Miryang 627-706, South Korea

[⊥]Energy Nano Materials Research Center, Korea Electronics Technology Institute (KETI), 68 Yatap-dong, Bundang-gu, Seongnam-si, Gyeonggi-do 463-816, Republic of Korea

[∥]Department of Physics and Centre for Plastic Electronics, Imperial College London, Prince Consort Road, London, SW7 2AZ, United Kingdom

[▽]Interdisciplinary School of Green Energy, Ulsan National Institute of Science and Technology (UNIST), Banyeon-ri 100, Ulsan 689-798, Republic of Korea

[○]Department of Materials Science and Engineering, KAIST, Daejeon 305-701, South Korea

Supporting Information

**ABSTRACT:** Highly efficient inverted-type red-emitting hybrid polymeric light-emitting diodes (HyPLEDs) were successfully demonstrated via Förster resonance energy transfer (FRET) and interfacial engineering of metal oxide with a cationic conjugated polyelectrolyte (CPE). Similarly structured green- and red-emissive polyfluorene copolymers, F8BT and F8TBT, were homogeneously blended as a FRET donor (host) and acceptor (dopant). A cationic polyfluorene-based CPE was also used as an interfacial layer for optimizing the charge injection/transport and improving the contact problem between the hydrophilic ZnO and hydrophobic polymer layer. A long Förster radius ($R_0$ = 5.32 nm) and high FRET efficiency (~80%) was calculated due to the almost-perfect spectral overlap between the emission of F8BT and the absorption of F8TBT. A HyPLED containing 2 wt % F8TBT showed a pure red emission ($\lambda_{max}$ = 640 nm) with a CIE coordinate of (0.62, 0.38), a maximum luminance of 26 400 cd/m$^2$ (at 12.8 V), a luminous efficiency of 7.14 cd/A (at 12.8 V), and a power efficiency of 1.75 lm/W (at 12.8 V). Our FRET-based HyPLED realized the one of the highest luminous efficiency values for pure red-emitting fluorescent polymeric light-emitting diodes reported so far.

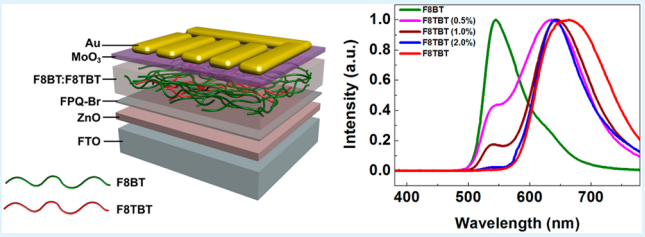


**KEYWORDS:** *energy transfer, hybrid polymer light-emitting diodes (HyPLEDs), red emission, F8BT, F8TBT*

## INTRODUCTION

Over the past two decades, conjugated polymer-based light-emitting diodes (PLEDs) have been extensively exploited for full-color flat-panel displays, solid-state lighting, and flexible optoelectronics, because of their low cost, facile color tunability by chemical structure modification, solution processability, large area fabrication, and mechanical flexiblility.[1−4]

The balanced device efficiency and lifetime of R-G-B light emissions are required to realize full-color display devices as a commercial product. However, both color purity and device efficiency of red-emissive PLEDs are still far behind those of green-emissive PLEDs. Several approaches have been suggested to realize red-light emission. A main strategy contains a chemical synthesis by combining a low-band-gap red-emitting moiety (such as 2,1,3-benzothiadiazole[5,6] and 2,1,3-benzoselenadiazole derivatives,[6,7] etc.) into a polymeric main chain, side chains, or end groups. In particular, the optical and electrical properties of polyfluorene (PFO)-based polymers can be easily controlled by the modification of chemical structure and red emission can be realized through introduction of comonomers into the PFO backbone, such as 4,7-bis(2-thienyl)-2,1,3-benzothiadiazole (TBT).[8] However, the red-emitting structures

Received: March 26, 2013
Accepted: May 23, 2013
Published: May 23, 2013

  

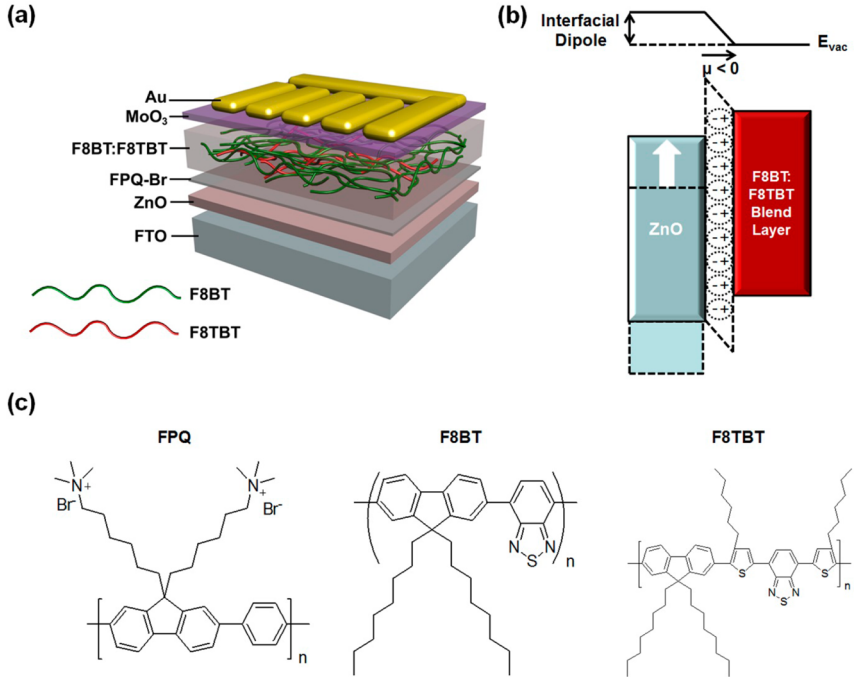


**Figure 1.** (a) Device structure of HyPLEDs. (b) Energy-level diagram of ZnO/FPQ/F8BT:F8TBT. (c) Chemical structure of FPQ, F8BT, and F8TBT.

often show a poor photoluminescence quantum yield (PLQY), due to strong intermolecular interactions, via dipole−dipole coupling and/or $\pi-\pi$ stacking, which leads to exciton quenching in a solid state.[9] Thus, most previously reported red-emissive PLEDs have shown poor luminance efficiency (less than ∼2.0 cd/A).[10−13] Attachment of a red-emissive moiety to the side chain of a PFO host was suggested to avoid the problems of phase separation and concentration quenching.[14,15] Recently, Chen et al. reported red-emitting PLED based on a doped polymer system with PFO as a host and 2,1,3-benzothiadiazole derivatives as a red dopant, showing a luminance efficiency of 5.50 cd/A, which is the highest efficiency for pure red-emitting PLEDs until now.[15]

The other universal method employs the polymer blend system, which is obtained by mixing a red-emitting polymer (or fluorophore) with a green-emitting host polymer, such as a polymer−polymer blend, polymer−small-molecule blend, and polymer−inorganic-complex blend, where efficient red emission can be realized via Förster resonance energy transfer (FRET).[16−19] However, polymer blend system has several problems, such as poor color stability caused by phase separation, the change of emission spectra with high bias voltage, and difficulties in fine-tuning the emission color. If dopant materials are uniformly dispersed in a host matrix, exciton quenching and poor color stability can be minimized. Moreover, the shift of emission spectrum toward a longer wavelength via FRET prevents overlap between absorption and emission spectra with decreased self-absorption. The effective dopant concentration has been reported to be no greater than 2% ± 0.5% (by weight).[16]

Conjugated polyelectrolytes (CPEs) with amphiphilic characteristics have been successfully utilized as an effective charge transport layer in organic optoelectronic devices.[20,21] The preference for the CPE polymer backbone to interact with the hydrophobic organic interface leads to generation of the spontaneously oriented interfacial dipoles. This can modify the electronic structures, shift the vacuum level and electrical contact at the interfaces, lower the energy barrier for charge injection/transport, and reduce the interfacial resistance between the hydrophilic metal oxide and hydrophobic active layers.

Here, we report a highly efficient red-emissive PLED via FRET using a homogeneous polymer blend of poly(9,9′-dioctylfluorene-co-2,1,3-benzothiadiazole) (F8BT) and poly[9,9′-dioctylfluorene-co-(4,7-bis(4-hexyl-2-thienyl)-2,1,3-benzothiadiazole)] (F8TBT). The two polymers are well-miscible to minimize phase separation due to the structural similarity based on the same polyfluorene backbone. The air-stable inverted-type organic−inorganic hybrid PLED (HyPLED) with a FTO/ZnO/F8BT:F8TBT/$MoO_3$/Au configuration showed a red emission with a CIE coordinate (0.62, 0.38) and a luminous efficiency of 7.14 cd/A. The surface of the ZnO layer was modified with a cationic conjugated polyelectrolyte (CPE), poly(9,9′-bis(6″-*N*,*N*,*N*-trimethylammoniumhexyl)fluorene-alt-phenylene) with bromide counterions (FPQ-Br) for efficient electron transport and hole blocking in the inverted PLEDs. Our HyPLED based on homogeneous polymer blends demonstrated the highest luminous efficiency among the pure red-emitting fluorescent PLEDs reported so far, through efficient FRET and interface engineering with the CPE layer.

## EXPERIMENTAL SECTION

**Synthesis of F8TBT.** 2,7-Bis(4,4,5,5-tetramethyl-1,3,2-dioxaborolan-2-yl)-9,9-dioctylfluorene (0.200 mmol, 0.129 g), 4,7-bis(5-bromo-4-hexyl-2-thienyl)-2,1,3-benzothiadiazole (0.200 mmol, 0.125 g), and $Pd(PPh_3)_4$ (3 mol %) were dissolved in a degassed mixture of toluene (6.0 mL) and aqueous 2 M $K_2CO_3$ solution (2.5 mL). The reaction mixture was stirred at 90 °C overnight. The mixture was precipitated into methanol and stirred for 2 h. The crude polymer was purified by Soxhlet extraction (with acetone and chloroform) and short column chromatography. Yield: 0.14 g (80%). $^1$H NMR (300 MHz, $CDCl_3$) $\delta$ (ppm): 8.07 (s, 2H), 7.98 (s, 2H), 7.79 (d, 2H), 7.55 (d, 2H), 7.52 (s, 2H), 2.83 (br, 4H) 2.06 (br, 4H), 1.77 (br, 4H), 1.49−1.13 (m, 36H),


dx.doi.org/10.1021/am401090m | ACS Appl. Mater. Interfaces 2013, 5, 5690−5695

0.89−0.79 (m, 12H). Number-average molecular weight (by gel permeation chromatography (GPC) in $CHCl_3$), $M_n$ = 16 000 g $mol^{-1}$ (PDI = 1.9).

**Synthesis of CPE.** The CPE (FPQ-Br) was synthesized by modifying the previously reported procedures.[30] $^1H$ NMR (300 MHz, DMSO) $\delta$ (ppm): 8.00−7.74 (br, 10H), 3.17 (br, 4H), 2.96 (s, 18H), 2.19 (br, 4H), 1.50 (br, 4H), 1.10 (br, 8H), 0.72 (br, 4H).

**Fabrication of IPLEDs.** FTO substrates were cleaned by sequential ultrasonication in acetone and isopropyl alcohol (IPA), and dried under a $N_2$ stream. An 80-nm-thick *n*-type ZnO layer was prepared by spray pyrolysis deposition from 80 mg $mL^{-1}$ zinc acetate dihydrate/methanol precursor solutions at 400 °C. The CPE layer was spin-coated on top of the ZnO layer from a methanol solution (0.1 wt %) and then annealed at 120 °C for 10 min to remove residual methanol. A 350-nm-thick F8BT:F8TBT emissive layer was spin-coated from *p*-xylene solutions (35 mg $mL^{-1}$) onto the CPE-modified ZnO surface, and then thermal annealing was performed at 155 °C for 1 h under a nitrogen atmosphere. A 10-nm-thick $MoO_3$ layer and a 70-nm-thick gold layer were subsequently evaporated on the emissive layer to complete the device fabrication.

**Atomic Force Microscopy (AFM).** The surface morphology of the pure F8BT film and F8BT:F8TBT blended film were characterized by atomic force microscopy (AFM). The AFM images (5 $\mu$m × 5 $\mu$m) were measured by a Veeco AFM microscope in tapping mode.

**Absorption and Photoluminescence (PL) Characterization.** The ultraviolet−visible (UV-Vis) absorption spectrum is obtained via UV−vis spectrometry (Varian Cary 5000). The photoluminescence spectra of F8BT and F8BT:F8TBT blended films on a quartz substrate were obtained on a Cary Eclipse spectrofluorometer with a xenon lamp as an excitation source (Edinburgh Instruments, Ltd.).

**Time-Correlated Single Photon Counting (TCSPC) Characterization.** The exciton lifetime was determined by the time-correlated single photon counting (TCSPC) technique. The details are shown in ref 3.

## RESULTS AND DISCUSSION

Figure 1a shows a HyPLED device configuration based on the homogeneous F8BT:F8TBT blend as an active electro-

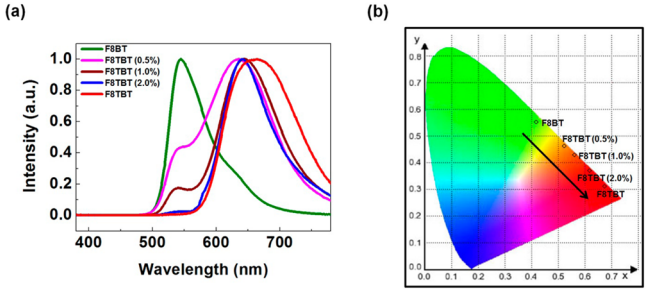


**Figure 2.** (a) Normalized electroluminescence (EL) spectra for a series of FTO/ZnO/FPQ/F8BT:F8TBT/$MoO_3$/Au devices with different F8TBT concentrations (expressed as wt %). (b) CIE chromaticity diagram for a series of FTO/ZnO/FPQ/F8BT:F8TBT/$MoO_3$/Au devices with different F8TBT concentrations (expressed as wt %).

luminescent layer. The device was prepared by sequential deposition of ZnO (electron injection layer), FPQ-Br (electron transport and hole blocking layer), F8BT:F8TBT (emissive active layer), $MoO_3$ (hole injection layer), and Au (anode) on a FTO transparent electrode/glass substrate (cathode).

Recently, $MoO_3$ deposited on gold demonstrated an unprecedented ohmic hole injection into a green-light-emitting polymer, F8BT.[22,23] In contrast, electron injection is much poorer than hole injection in HyPLEDs, because of the large contact barrier between the conduction band of ZnO (~4.0

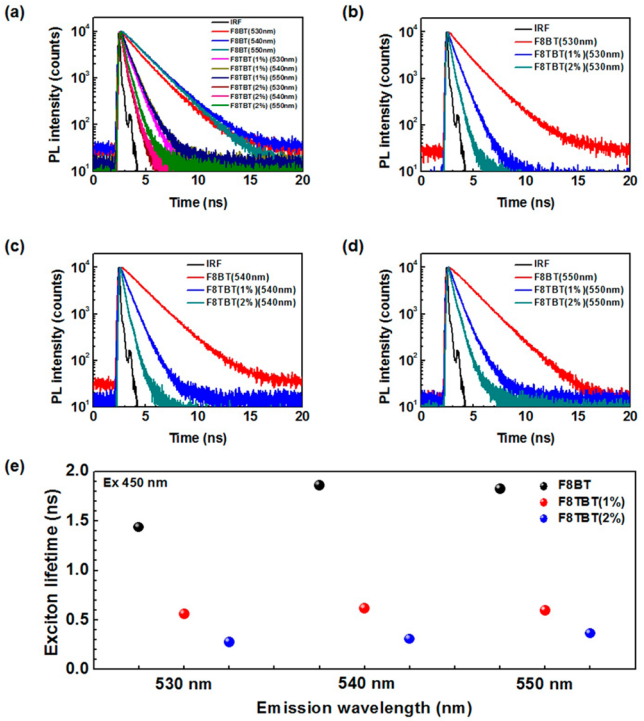


**Figure 3.** (a) Time-resolved PL signals of F8BT, F8TBT (1%), and F8TBT (2%) films, measured by time-correlated single photon counting (TCSPC) at emission wavelengths of 530-550 nm. (b−d) Time-resolved PL signals of F8BT, F8TBT (1%), and F8TBT (2%) films, measured by time-correlated single photon counting (TCSPC) at specific emission wavelengths of (b) 530 nm, (c) 540 nm, and (d) 550 nm. (e) Exciton lifetime of F8BT, F8TBT (1%), and F8TBT (2%) films.

**Table 1. Summarized Exciton Lifetime of F8BT, F8TBT (1%), and F8TBT (2%) Films**[a]

| film configuration | $\tau_{avr}$ [ns] | $\eta$ [%] |
|---|---|---|
| **530 nm Emission** | | |
| quartz/F8BT | 1.44 | |
| quartz/F8BT(99%):F8TBT(1%) | 0.56 | 61.1 |
| quartz/F8BT(98%):F8TBT(2%) | 0.28 | 80.6 |
| **540 nm Emission** | | |
| quartz/F8BT | 1.86 | |
| quartz/F8BT(99%):F8TBT(1%) | 0.62 | 66.7 |
| quartz/F8BT(98%):F8TBT(2%) | 0.31 | 83.3 |
| **550 nm Emission** | | |
| quartz/F8BT | 1.82 | |
| quartz/F8BT(99%):F8TBT(1%) | 0.60 | 67.0 |
| quartz/F8BT(98%):F8TBT(2%) | 0.36 | 80.2 |

[a] $\lambda_{Ex}$ = 450 nm.

eV)[21,24,25] and the lowest unoccupied molecular orbital (LUMO) of F8BT (~3.0 eV).[20,24] Consequently, electron and hole injections are unbalanced and their recombination probability is also low in HyPLEDs without interfacial engineering. In our previous study, we have successfully demonstrated an ideal surface engineering and highly efficient HyPLEDs by introducing the CPE layer (FPQ-Br) on top of the metal oxide as an electron transport layer (ETL) and hole blocking layer (HBL).[21] Spontaneously aligned interfacial dipoles within the interfacial CPE layer between metal oxide and organic semiconductor layers offered the reduced injection

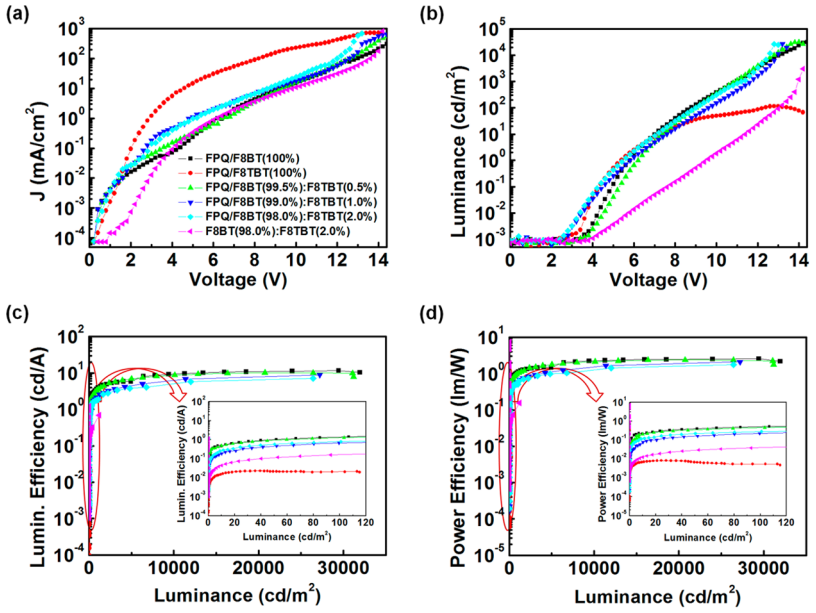


**Figure 4.** HyPLEDs characterization of (a) current density versus voltage ($J$–$V$), (b) luminance versus voltage ($L$–$V$), (c) luminous efficiency versus luminance ($E$–$L$), and (d) power efficiency versus luminance ($P$–$L$).

**Table 2. Summarized Device Performances of HyPLEDs with Different F8TBT Concentrations**

| device configuration | $L_{max}$ [cd/m$^2$] @ bias | LE$_{max}$ [cd/A] @ bias | PE$_{max}$ [lm/W] @ bias | EQE$_{max}$ [%] @ bias |
|---|---|---|---|---|
| FTO/ZnO/FPQ/F8BT(100%)/$MoO_3$/Au | 32000 (14.4 V) | 11.60 (14.2 V) | 2.57 (14.2 V) | 3.4 |
| FTO/ZnO/FPQ/F8TBT(100%)/$MoO_3$/Au | 120 (12.8 V) | 0.023 (9.2 V) | 0.0082 (8.4 V) | 2.8 |
| FTO/ZnO/FPQ/F8BT(99.5%):F8TBT(0.5%)/$MoO_3$/Au | 31200 (14.0 V) | 10.14 (13.4 V) | 2.38 (13.4 V) | 3.0 |
| FTO/ZnO/FPQ/F8BT(99.0%):F8TBT(1.0%)/$MoO_3$/Au | 27200 (13.2 V) | 8.82 (13.2 V) | 2.10 (13.2 V) | 2.8 |
| FTO/ZnO/FPQ/F8BT(98.0%):F8TBT(2.0%)/$MoO_3$/Au | 26400 (12.8 V) | 7.14 (12.8 V) | 1.75 (12.8 V) | 2.8 |
| FTO/ZnO/F8BT(98.0%):F8TBT(2.0%)/$MoO_3$/Au | 3030 (14.2 V) | 0.69 (14.0 V) | 0.15 (14.0 V) | 3.8 |

barrier for electrons as well as effective hole blocking. Although perfectly balanced carrier injection was not fully achieved, it provided a new opportunity to maximize the electron–hole recombination probability in the active layer.

Figure 1b shows the schematic energy level diagram of the ZnO/FPQ-Br/F8BT:F8TBT blend layer employed in this study. (A full energy diagram including F8BT and F8TBT is provided in Figure S1 in the Supporting Information.) The spontaneous negative dipole in the FPQ-Br CPE layer pointing away from the ZnO interface would effectively shift the band edge of the ZnO closer to the vacuum level of the polymer blend layer.[20,21] The self-aligned interfacial dipoles at the CPE/ZnO interface were confirmed by measuring the temporal time response of current density and luminance for FTO/ZnO/150-nm-thick F8BT(98%):F8TBT(2%)/$MoO_3$/Au with (line formed by solid red circles) and without CPE (line formed by solid black squares) layer under a forward bias of 8.0 V. The current density and luminance under a constant forward bias of 8.0 V did not show significant changes with time, as shown in Figure S2 in the Supporting Information.

The chemical structures of FPQ-Br, F8BT, and F8TBT are shown in Figure 1c. It is well-known that F8BT is a highly efficient green emitter particularly in HyPLEDs.[20,21,26] A red-emitting polymer, F8TBT was designed and synthesized for blending with green-emitting F8BT as a dopant. F8BT and F8TBT are expected to have great compatibility (and miscibility) in common organic solvents because both structures have the same PFO-based main backbone.

F8BT was supplied from Cambridge Display Technology, Ltd. ($M_n$ = 114 kg mol$^{-1}$). F8TBT was synthesized following the previously reported procedures.[8] The monomer, 4,7-bis(5-bromo-4-hexyl-2-thienyl)-2,1,3-benzothiadiazole was prepared by palladium-catalyzed stille coupling between 4-(hexyl-2-thienyl)stanne and 4,7-dibromo-2,1,3-benzothiadiazole, followed by bromination with *N*-bromosuccinimide. The brominated monomer was polymerized with 2,7-bis(4,4,5,5-tetramethyl-1,3,2-dioxaborolan-2-yl)-9,9-dioctylfluorene via Suzuki polycondensation in 80% yield. The number-average molecular weight was measured to be 16 000 g mol$^{-1}$ (PDI: 1.9) via GPC, using chloroform as an eluent, relative to a polystyrene standard. The hexyl side chain on the thiophene moiety yielded good solution processability for device fabrication.[8]

The UV–vis absorption and PL spectra of F8TBT and F8BT are shown in Figure S3 in the Supporting Information. The emission spectrum of F8BT ($\lambda_{max}$ = 540 nm) was almost perfectly overlapped the absorption spectrum of F8TBT ($\lambda_{max}$ = 550 nm) in film, where efficient FRET from the F8BT host to the F8TBT dopant is expected. The energy-transfer efficiency is also very sensitive to the intermolecular distance between the donor and acceptor molecules; thus, a homogeneous polymer blend without phase separation is crucial for enhanced device performance and long-term stability. In Figure S4 in the Supporting Information, atomic force microcopy (AFM) images of the F8BT:F8TBT blending film (98:2 (wt %)) showed no phase separation morphology, while the F8BT:F8TBT blend film (70:30 (wt %)) showed an aggregated


dx.doi.org/10.1021/am401090m | ACS Appl. Mater. Interfaces 2013, 5, 5690–5695

morphology. It supports the formation of homogeneous surface morphology with no visible phase separation in F8BT:F8TBT film (98:2 (wt %)).

Figure 2a represents the electroluminescence (EL) emission spectra of F8BT, F8TBT, and F8BT:F8TBT blended polymers with different F8TBT doping concentrations of 0.5, 1.0, and 2.0 wt %. EL emission spectra of the F8BT:F8TBT blends changed with the F8TBT dopant concentration. As the concentration of F8TBT increased, the typical spectral characteristics of F8BT disappeared and that of the red F8TBT emission ($\lambda_{max}$ = 640 nm) increased. At a doping concentration of 2 wt %, almost-pure red emission was measured via complete FRET from F8BT to F8TBT. The EL emission spectrum of the homogeneous F8BT:F8TBT blend film (98:2 (wt %)) was much narrower than that of pure F8TBT, because of a solid-solution state effect that the polymer F8TBT was uniformly dispersed in the F8BT host polymer matrix as existing in solution state and the intermolecular interactions are significantly reduced by dilution effects.[19] This behavior was also shown in the CIE coordinates in Figure 2b. The CIE (1931) coordinates of F8BT, F8TBT, and F8BT:F8TBT blends with F8TBT concentrations of 0.5, 1.0, and 2.0 wt % in HyPLEDs, were determined to be ($X$ = 0.42, $Y$ = 0.56), ($X$ = 0.68, $Y$ = 0.31), ($X$ = 0.52, $Y$ = 0.47), ($X$ = 0.57, $Y$ = 0.43), and ($X$ = 0.62, $Y$ = 0.38), respectively. The color coordinates dramatically moved toward a pure red emission with the addition of a small amount of F8TBT into the F8BT matrix.

The spectral changes with different doping content of F8TBT were analyzed by dipole−dipole Förster energy transfer from F8BT to F8TBT. The Förster radius ($R_0$) is defined as the distance between the donor and the acceptor materials at which the probability of intermolecular energy transfer equals that of the donor relaxation via fluorescence. This means that the exciton on F8TBT is as likely to decay (either radiatively or nonradiatively) as it is to decay on F8BT. $R_0$ can be calculated from the spectral overlap of the emission of donor and absorption of acceptor via eq 1:[18,27]

$$(R_0)^6 = \left(\frac{0.5291K^2}{N_A n^4}\right)T \tag{1}$$

where $K^2$ is an orientation factor (2/3 for random orientation), $N_A$ is Avogadro's number, and $n$ is the refractive index of the host. $T$ is the overlap integral between the absorption spectrum of the acceptor and the fluorescence spectrum of the donor, which is defined as follows:

$$T = \int_0^\infty F_m(\bar{\nu})\varepsilon_Q(\bar{\nu})\frac{d\nu}{\bar{\nu}^4} \tag{2}$$

where $F_m$ is the normalized fluorescence spectrum of the donor, and $\varepsilon_Q$ is the molar extinction coefficient of the acceptor, both expressed as a function of energy in wavenumbers ($\bar{\nu}$).

For our F8BT:F8TBT blend system, a large value of $R_0$ was calculated (5.32 nm), which comes from the almost-perfect overlap between the emission of F8BT and the absorption of F8TBT, leading to very efficient Förster energy transfer. Moreover, the FRET efficiency was also measured by time-correlated single-photon counting (TCSPC) technique, according to eq 3:[28,29]

$$E_{FRET} = 1 - \frac{\tau_{DA}}{\tau_D} \tag{3}$$

where $\tau_{DA}$ is the exciton lifetime of the donor in the presence of the acceptor and $\tau_D$ is the lifetime of the donor alone (without acceptor). The average exciton lifetime of the donor, F8BT, was determined to be 1.4−1.8 ns. The lifetime of the blended films decreased up to ∼0.6 ns at [F8TBT] = 1 wt % and ∼0.3 ns at [F8TBT] = 2 wt %. As the doped concentration of F8TBT (acceptor) increased, the exciton lifetime of F8BT decreased, because of the additional fast pathway for deactivation of the excited states via efficient FRET to F8TBT (Figure 3). The resulting FRET efficiency was calculated to be ∼60% and ∼80% for the F8BT(99%):F8TBT (1%) and F8BT(98%):F8TBT (2%) blended systems, respectively. The detailed liftetime data are summarized in Table 1.

The detailed EL characteristics of F8BT, F8TBT, and F8BT:F8TBT in HyPLEDs were investigated by (a) current density versus applied voltage ($J$−$V$), (b) luminance versus applied voltage ($L$−$V$), (c) luminous efficiency versus luminance ($E$−$L$), and (d) power efficiency versus luminance ($P$−$L$), as shown in Figure 4. The F8TBT-based HyPLED was fabricated as a reference, showing a maximum luminance of 120 cd/m$^2$ (at 12.8 V), luminous efficiency of 0.023 cd/A (at 9.2 V), and power efficiency of 0.0082 lm/W (at 8.4 V). In contrast, HyPLEDs containing a polymer blend with 2 wt % F8TBT showed the ideal red emission ($\lambda_{max}$ = 640 nm) and dramatically enhanced EL performance with a maximum luminance of 26 400 cd/m$^2$ (at 12.8 V), a luminous efficiency of 7.14 cd/A (at 12.8 V), and a power efficiency of 1.75 lm/W (at 12.8 V), showing ca. 200−300-fold enhanced luminous characteristics, compared to the reference HyPLED. This high device efficiency in inverted-type red-emitting HyPLEDs originates from effective FRET with a large value of $R_0$ (5.32 nm) and interfacial engineering of metal oxide layer with the CPE. Details of the device characteristics are shown in Table 2.

Moreover, the air stability of HyPLEDs with a homogeneous F8BT:F8TBT blending system was evaluated under ambient atmospheric conditions without further encapsulation (see Figures S5(a)−(c) in the Supporting Information). The luminance and luminous efficiency of the device were measured at 100 cd/m$^2$ for 100 h. Despite the long exposure to the air, the normalized luminance and luminous efficiency for 100 h were maintained almost uniformly, compared to those of their initial state. In Figure S5(d) in the Supporting Information, the spectra of HyPLEDs with homogeneous F8BT:F8TBT blending films were similar with increased luminance. However, the spectra of HyPLEDs using F8BT:Merck-red and F8BT:P3HT blending films with different polymer backbones changed as the luminance increased, as shown in Figures S5(e) and S5(f) in the Supporting Information. Therefore, we confirm that the HyPLEDs with a homogeneous F8BT:F8TBT blending film show long-term stability of the desired donor−acceptor nanomorphology.

## CONCLUSION

In conclusion, we demonstrated a highly efficient red-emitting hybrid polymeric light-emitting diodes (HyPLED) via Förster energy transfer with the homogeneous polymer blend of similarly structured F8BT and F8TBT based on a same polyfluorene conjugated backbone. Inverted-type device architecture was utilized with zinc oxide/conjugated polyelectrolyte (ZnO/CPE) as an electron injection/transport layer to optimize the EL characteristics of HyPLED. A large Förster radius of $R_0$ = 5.32 nm was determined due to the almost-perfect spectral overlap between the emission of F8BT and

absorption of F8TBT as a FRET donor and acceptor, respectively, resulting in efficient Förster resonance energy transfer (FRET)-mediated red emission (FRET efficiency ≈ 80%). The inverted PLED based on F8BT:F8TBT (98:2 (wt %)) showed a red emission (CIE coordinate = (0.62, 0.38), $\lambda_{max}$ = 640 nm) with the maximum luminance of 26 400 cd/m$^2$, a luminous efficiency of 7.14 cd/A, and a luminance turn-on voltage of 2.8 V. To the best of our knowledge, the luminous efficiency obtained here is the one of the highest values for pure red-emissive polymeric light-emitting diodes reported so far.

## ■ ASSOCIATED CONTENT

### Supporting Information

Full energy diagram of HyPLEDs; time response of current density and luminance; normalized absorption photoluminescence spectra of F8BT and F8TBT; AFM images (pure F8BT film and F8BT:F8TBT blending films with different weight percentages of F8TBT in the F8BT host); the air stability of HyPLEDs (PDF). This material is available free of charge via the Internet at http://pubs.acs.org.

## ■ AUTHOR INFORMATION

### Corresponding Author

*Tel.: +82 52 217 2316 (M.H.S.), +82 55 350 5300 (H.Y.W.). Fax: +82 52 217 2309 (M.H.S.), +82 55 350 5837 (H.Y.W.). E-mail: mhsong@unist.ac.kr (M.H.S.), hywoo@pusan.ac.kr (H.Y.W.).

### Notes

The authors declare no competing financial interest.

## ■ ACKNOWLEDGMENTS

We thank Cambridge Display Technology (CDT) for providing us with F8BT polymer. This work was supported by the National Research Foundation of Korea (NRF) grant (No. 2012R1A2A2A06046931) by the Ministry of Science, ICT & Future Planning (MSIP). This study was also supported by the NRF grant (Nos. 2012R1A1A2005855, R31-2008-000-20004-0, 2009-0093020) by the Ministry of Education, Science and Technology, Korea.

## ■ REFERENCES

(1) Burroughes, J. H.; Bradley, D. D. C.; Brown, A. R.; Marks, R. N.; Mackay, K.; Friend, R. H.; Burns, P. L.; Holmes, A. B. *Nature* **1990**, *347*, 539−541.
(2) D'Andrade, B. W.; Forrest, S. R. *Adv. Mater.* **2004**, *16*, 1585−1595.
(3) Lee, B. R.; Kim, J. W.; Kang, D.; Lee, D. W.; Ko, S. J.; Lee, H. J.; Lee, C. L.; Kim, J. Y.; Shin, H. S.; Song, M. H. *ACS Nano* **2012**, *6*, 2984−2991.
(4) Hwang, J. O.; Park, J. S.; Choi, D. S.; Kim, J. Y.; Lee, S. H.; Lee, K. E.; Kim, Y. H.; Song, M. H.; Yoo, S.; Kim, S. O. *ACS Nano* **2012**, *6*, 159−167.
(5) Hou, Q.; Zhou, Q. M.; Zhang, Y.; Yang, W.; Yang, R. Q.; Cao, Y. *Macromolecules* **2004**, *37*, 6299−6305.
(6) Yang, R. Q.; Tian, R. Y.; Yan, J. G.; Zhang, Y.; Yang, J.; Hou, Q.; Yang, W.; Zhang, C.; Cao, Y. *Macromolecules* **2005**, *38*, 244−253.
(7) Yang, R. Q.; Tian, R. Y.; Hou, Q.; Yang, W.; Cao, Y. *Macromolecules* **2003**, *36*, 7453−7460.
(8) Zaumseil, J.; McNeill, C. R.; Bird, M.; Smith, D. L.; Ruden, P. P.; Roberts, M.; McKiernan, M. J.; Friend, R. H.; Sirringhaus, H. *J. Appl. Phys.* **2008**, *103*, 064517.
(9) Chen, C. T. *Chem. Mater.* **2004**, *16*, 4389−4400.
(10) Cho, N. S.; Hwang, D. H.; Jung, B. J.; Lim, E.; Lee, J.; Shim, H. K. *Macromolecules* **2004**, *37*, 5265−5273.
(11) Cho, N. S.; Park, J. H.; Lee, S. K.; Lee, J.; Shim, H. K.; Park, M. J.; Hwang, D. H.; Jung, B. J. *Macromolecules* **2006**, *39*, 177−183.
(12) Wang, E. G.; Li, C.; Zhuang, W. L.; Peng, J. B.; Cao, Y. *J. Mater. Chem.* **2008**, *18*, 797−801.
(13) Park, M. J.; Lee, J.; Jung, I. H.; Park, J. H.; Hwang, D. H.; Shim, H. K. *Macromolecules* **2008**, *41*, 9643−9649.
(14) Liu, J.; Chen, L.; Shao, S. Y.; Xie, Z. Y.; Cheng, Y. X.; Geng, Y. H.; Wang, L. X.; Jing, X. B.; Wang, F. S. *J. Mater. Chem.* **2008**, *18*, 319−327.
(15) Chen, L.; Zhang, B. H.; Cheng, Y. X.; Xie, Z. Y.; Wang, L. X.; Jing, X. B.; Wang, F. S. *Adv. Funct. Mater.* **2010**, *20*, 3143−3153.
(16) Tang, C. W.; Vanslyke, S. A.; Chen, C. H. *J. Appl. Phys.* **1989**, *65*, 3610−3616.
(17) McNeill, C. R.; Greenham, N. C. *Adv. Mater.* **2009**, *21*, 3840−3850.
(18) Virgili, T.; Lidzey, D. G.; Bradley, D. D. C. *Adv. Mater.* **2000**, *12*, 58−62.
(19) Liu, J.; Shi, Y. J.; Yang, Y. *Appl. Phys. Lett.* **2001**, *79*, 578−580.
(20) Choi, H.; Park, J. S.; Jeong, E.; Kim, G. H.; Lee, B. R.; Kim, S. O.; Song, M. H.; Woo, H. Y.; Kim, J. Y. *Adv. Mater.* **2011**, *23*, 2759−2763.
(21) Park, J. S.; Lee, B. R.; Jeong, E.; Lee, H. J.; Lee, J. M.; Kim, J. S.; Kim, J. Y.; Woo, H. Y.; Kim, S. O.; Song, M. H. *Appl. Phys. Lett.* **2011**, *99*, 163305.
(22) Nakayama, Y.; Morii, K.; Suzuki, Y.; Machida, H.; Kera, S.; Ueno, N.; Kitagawa, H.; Noguchi, Y.; Ishii, H. *Adv. Funct. Mater.* **2009**, *19*, 3746−3752.
(23) Hamwi, S.; Meyer, J.; Winkler, T.; Riedl, T.; Kowalsky, W. *Appl. Phys. Lett.* **2009**, *94*, 253307.
(24) Park, J. S.; Lee, B. R.; Lee, J. M.; Kim, J. S.; Kim, S. O.; Song, M. H. *Appl. Phys. Lett.* **2010**, *96*, 243306.
(25) Lee, B. R.; Choi, H.; SunPark, J.; Lee, H. J.; Kim, S. O.; Kim, J. Y.; Song, M. H. *J. Mater. Chem.* **2011**, *21*, 2051−2053.
(26) Kabra, D.; Lu, L. P.; Song, M. H.; Snaith, H. J.; Friend, R. H. *Adv. Mater.* **2010**, *22*, 3194−3198.
(27) Shoustikov, A.; You, Y. J.; Burrows, P. E.; Thompson, M. E.; Forrest, S. R. *Synth. Met.* **1997**, *91*, 217−221.
(28) Clapp, A. R.; Medintz, I. L.; Mauro, J. M.; Fisher, B. R.; Bawendi, M. G.; Mattoussi, H. *J. Am. Chem. Soc.* **2004**, *126*, 301−310.
(29) Sapsford, K. E.; Berti, L.; Medintz, I. L. *Angew. Chem., Int. Ed.* **2006**, *45*, 4562−4588.
(30) Hoven, C. V.; Garcia, A.; Bazan, G. C.; Nguyen, T. Q. *Adv. Mater.* **2008**, *20*, 3793−3810.